ChemPubSoc Europe

DOI: 10.1002/open.201800161

Open Access ChemistryOPEN Full Papers

Exploration of High-Energy-Density Materials: Computational Insight into Energetic Derivatives Based on 1,2,4,5-Tetrahydro-1,2,4,5-tetrazine

Xinghui Jin,*[a] Jianhua Zhou,[a] and Bingcheng Hu[b]

Density functional theory was employed to investigate ten 1,2,4,5-tetrahydro-1,2,4,5-tetrazine-based energetic materials. The heats of formation and detonation properties were calculated by isodesmic reactions and Kamlet–Jacobs equations. The thermal stabilities and impact sensitivities were also estimated to give a better understanding of their decomposition mechanism. The results indicate that all of the designed compounds have high positive heats of formation ranging from 525.1 to 1639.1 kJ mol^{-1}, moderate detonation properties (heats of detonation of 536.6 to 2187.6 cal g^{-1}, theoretical densities of 1.48 to 2.32 g cm^{-3}, detonation velocities of 7.02 to 12.18 km s^{-1}, and detonation pressures of 19.8 to 75.1 GPa), and acceptable stabilities (bond dissociation energies of 0.8 to 104.9 kJ mol^{-1}). Taking both the detonation properties and the stabilities into consideration, compounds **A4** and **B4** were finally selected as promising candidates of high-energy-density materials, as their detonation properties and impact sensitivities were superior to those of HMX. Additionally, the frontier molecular orbitals, electronic densities, electrostatic potentials, and thermal dynamic parameters of compounds **A4** and **B4** were also investigated.

1. Introduction

Energetic materials with high nitrogen contents have attracted significant attention because of their high positive heats of formation, excellent detonation properties, environmental acceptabilities, favorable insensitivities, and thermal stabilities.[1–4] The search for novel explosives, especially cyclic high-energy-density materials, has become one of the most active topics to meet future demands,[5] as these heterocycles contain a large number of inherently energetic C–N and N–N bonds. Not surprisingly, 1,2,4,5-tetrazine consists of this type of structure and has a nitrogen content of 68.3%. To our best knowledge, recent investigations of 1,2,4,5-tetrazine derivatives have mainly focused on introducing energetic groups to the carbon atoms by nucleophilic substitution reactions.[6–8] This is because the strong electrophilic effects of the nitrogen atoms reduce the electron density that is distributed on the carbon atoms, and then these carbon atoms easily attract nucleophilic reagents to form various 1,2,4,5-tetrazine-based energetic derivatives. However, each of these compounds has different advantages and disadvantages with respect to its stabilities and detonation properties. Taking 3,6-diazido-1,2,4,5-tetrazine as an example, its applications have been limited due to its notorious sensitivity to spark, friction, and impact as well as its thermal stability.[9] This led to question the properties that these new energetic materials would possess if the –N=N bonds in the 1,2,4,5-tetrazine ring were replaced by –NHNH– bonds. Consequently, two parent compounds were designed (Figure 1, compounds **A** and **B**). However, previous research also demonstrated that energetic groups such as $-NO_2$, $-NF_2$, $-NH_2$, $-NHNO_2$, and $-NHNH_2$ were effective structural units that could be used to improve the detonation properties of energetic compounds,[10] and finally, a series of 1,2,4,5-tetrahy-

[a] *Prof. Dr. X. Jin, Prof. Dr. J. Zhou*
School of Chemistry and Pharmaceutical Engineering
Qilu University of Technology (Shandong Academy of Sciences)
Ji'nan 250353 (China)
E-mail: jingetiema0000@126.com

[b] *Prof. Dr. B. Hu*
School of Chemical Engineering
Nanjing University of Science and Technology
Nanjing, 210094 (China)

The ORCID identification number(s) for the author(s) of this article can be found under: https://doi.org/10.1002/open.201800161.

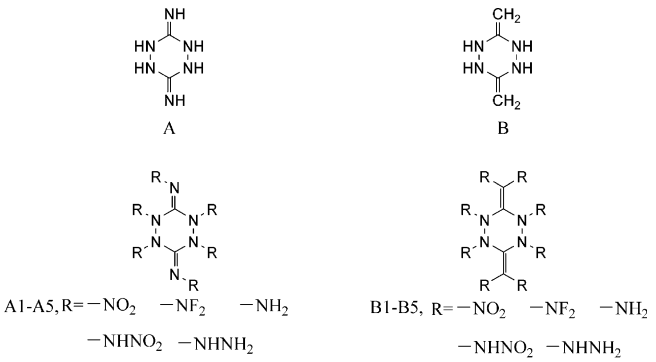

Figure 1. The designed parent molecules and energetic derivatives.

dro-1,2,4,5-tetrazine-based energetic materials were designed (Figure 1, compounds **A1–A5** and **B1–B5**).

In this work, we report the systematic investigation of the heats of formation, detonation properties, bond dissociation energies, and sensitivities of a series of 1,2,4,5-tetrahydro-1,2,4,5-tetrazine-based energetic molecules by density functional theory. Afterwards, the promising high-energy-density materials were screened on the basis of the calculated data, and their frontier molecular orbitals, electronic densities, electrostatic potentials, and thermal dynamic parameters were fully investigated. It is expected that our research will provide better understanding of the chemical and physical properties of these high-energy-density materials.

2. Results and Discussion

2.1. Heat of Formation

The total energies (E_0 [au]), zero-point energies (ZPEs [kJ mol^{-1}]), thermal corrections (H_T [kJ mol^{-1}]), and gas-phase heats of formation ($\Delta H_{f,gas}$ [kJ mol^{-1}]) of the reference compounds listed in the isodesmic reactions are summarized in Table 1. From this table it is found that both compounds **A** and **B** have high positive gas-phase heats of formation, which will make significant contributions to the solid-phase heats of formation of the designed compounds.

Table 2 lists the calculated total energies, thermal corrections, zero-point energies, gas-phase heats of formation, heats of sublimation (ΔH_{sub} [kJ mol^{-1}]), and solid-phase heats of formation ($\Delta H_{f,solid}$ [kJ mol^{-1}]) of the designed compounds. The molecular properties such as the molecular surface area (A), degree of balance between the positive and negative potentials on the isosurface (ν), and the measure of variability of the electrostatic potential on the molecular surface (σ^2_{tot}) are also presented. It is found that both series **A** and **B** have high positive gas-phase (ranging from 855.7 to 1800.1 kJ mol^{-1} and from 665.1 to 1266.8 kJ mol^{-1}, respectively) and solid-phase heats of formation (ranging from 747.0 to 1639.1 kJ mol^{-1} and from 525.1 to 1013.3 kJ mol^{-1}, respectively).

Figure 2a displays a comparison of the effects of different substituents on the gas-phase heats of formation of the designed compounds. It is found that all of the compounds that are substituted by energetic groups possess higher solid-phase heats of formation than the corresponding unsubstituted parent compounds, except for compound **B2**. The heats of formation of series **A** are also higher than those of corresponding

Table 1. Calculated total energies (E_0), zero-point energies (ZPE), thermal corrections (H_T), and heats of formation ($\Delta H_{f,gas}$) for the reference compounds.

Compd	E_0[a] [au]	ZPE[a] [kJ mol^{-1}]	H_T[a] [kJ mol^{-1}]	$\Delta H_{f,gas}$ [kJ mol^{-1}]
NH_3	−56.557769	90.4	10.0	−45.9[b]
CH_4	−40.524020	118.2	10.0	−74.6[b]
CH_3NHNH_2	−151.101622	214.0	14.2	94.5[b]
CH_3NF_2	−294.209863	123.7	13.6	−98.4[c]
CH_3NH_2	−95.863690	168.6	11.4	−23.5[b]
CH_3NHNO_2	−300.352337	177.5	16.1	−8.4[c]
CH_3NO_2	−245.013375	131.4	13.8	−81.0[b]
NH_2NHNH_2	−167.194269	185.0	13.5	206.8[c]
NH_2NF_2	−310.230386	93.7	13.2	−12.7[c]
NH_2NH_2	−111.868658	140.0	11.1	104.2[c]
NH_2NHNO_2	−316.355111	147.1	15.5	119.1[c]
NH_2NO_2	−261.035046	100.6	11.7	−6.4[c]
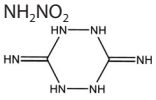	−408.222579	278.0	17.5	493.5[c]
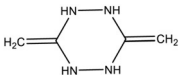	−376.087129	331.4	18.4	554.6[c]

[a] Calculated at the B3LYP/6-31G(d,p) level. [b] Obtained from http://webbook.nist.gov. [c] Calculated at the CBS-Q level.

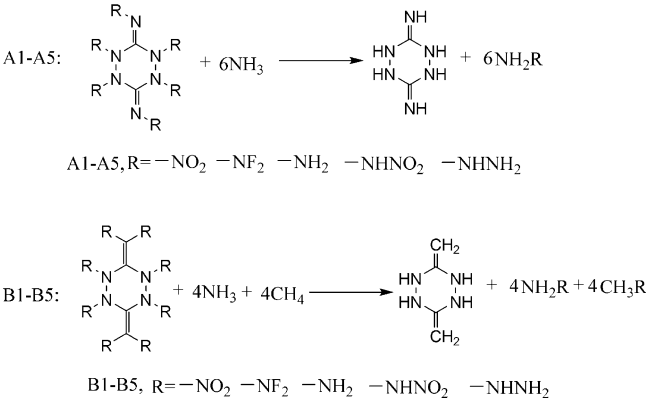

Figure 2. Variation trends of the heats of formation of the designed compounds.

Table 2. Calculated total energies, thermal corrections, zero-point energies, molecular properties, and heats of formation of the designed compounds.

Compd	E_0 [au]	ZPE [kJ mol^{-1}]	H_T [kJ mol^{-1}]	$\Delta H_{f,gas}$ [kJ mol^{-1}]	A [Å]	ν	σ^2_{tot} [(kcal mol^{-1})^2]	ΔH_{sub} [kJ mol^{-1}]	$\Delta H_{f,solid}$ [kJ mol^{-1}]
A1	−1635.003201	305.9	64.3	951.8	297.3	0.055	212.5	134.8	817.0
A2	−1930.192417	259.1	65.5	855.7	272.6	0.12	30.5	108.7	747.0
A3	−740.166791	550.6	40.9	1178.8	217.0	0.23	197.4	111.6	1067.2
A4	−1967.019798	581.3	78.2	1439.7	357.6	0.087	237.4	186.7	1253.0
A5	−1072.119393	818.9	59.9	1800.1	306.3	0.25	160.3	161.0	1639.1
B1	−2011.897886	380.9	78.3	827.2	341.9	0.051	227.2	166.6	660.6
B2	−2405.488196	316.9	82.2	665.1	324.5	0.056	37.0	140.0	525.1
B3	−818.867239	703.9	48.0	884.5	247.1	0.18	234.4	125.5	759.0
B4	−2454.66518	748.0	97.6	1266.8	437.4	0.06	260.3	253.5	1013.3
B5	−1261.422853	1063.9	73.7	978.8	339.4	0.25	188.1	188.5	790.3

series **B**, because the former contains a larger number of energetic C=N chemical bonds. Besides, the heats of formation for series **A** follow the order $-NF_2 < -NO_2 < -NH_2 < -NHNO_2 < -NHNH_2$, whereas those for series **B** follow the order $-NF_2 < -NO_2 < -NH_2 < -NHNH_2 < -NHNO_2$. It can be concluded that the $-NHNH_2$ group is effective in improving the heats of formation of series **A**, whereas the $-NHNO_2$ group plays an important role in improving the heats of formation of series **B**. Overall, the $-NF_2$ group contributes the least to improving the heats of formation for both series **A** and **B**. A comparison of the gas-phase and solid-phase heats of formation of the designed compounds is also presented in Figure 2b. Clearly, the variation trends in the solid-phase heats of formation are the same as those observed for the gas-phase heats of formation. This phenomenon reveals that the variation trends of the heats of formation under the influence of different substituents drawn from the gas-phase results are consistent with those drawn from the solid-phase ones.

2.2. Detonation Properties

The heats of detonation (Q), densities (ρ), detonation velocities (D), and detonation pressures (P) were predicted accurately, as these parameters are critical indicators in evaluating the detonation properties of energetic compounds. Table 3 lists the systemic data of the designed compounds and two famous explosives (RDX and HMX) for comparison. It can be found from Table 3 that most of the designed compounds have high positive heats of detonation (series **A**: from 998.3 to 2187.6 cal g^{-1}; series **B**: from 536.6 to 2137.9 cal g^{-1}), high densities (series **A**: from 1.52 to 2.29 g cm^{-3}; series **B**: from 1.48 to 2.32 g cm^{-3}), and acceptable detonation properties (series **A**: D = 8.47–12.18 km s^{-1}, P = 29.8–75.1 GPa; series **B**: D = 7.02–12.08 km s^{-1}, P = 29.8–74.3 GPa).

Figure 3 displays the variation trends of Q, ρ, D, and P of the designed compounds, and the data for RDX and HMX are also presented for visual comparison. It can be seen that the heats of detonation of series **A** follow the order $-NO_2 < -NH_2 < -NHNH_2 < -NHNO_2 < -NF_2$, whereas those of series **B** follow the order $-NHNH_2 < -NH_2 < -NO_2 < -NHNO_2 < -NF_2$. Compounds that are substituted with a $-NF_2$ group possess higher heats of detonation (compound **A2**, 2187.6 cal g^{-1}; compound **B2**, 2137.9 cal g^{-1}) than HMX (1633.9 cal g^{-1}). This indicates that the $-NF_2$ group is the most favorable for improving the heats of detonation of the designed molecules. Among the ten compounds, six compounds (**A1**, **A2**, **A4**, **B1**, **B2**, and **B4**) have higher densities than RDX (1.82 g cm^{-3}) and four compounds (**A1**, **A2**, **B1**, and **B2**) have higher densities than HMX (1.91 g cm^{-3}).[11] The density data of series **A** follow the order $-NHNH_2 < -NH_2 < -NHNO_2 < -NO_2 < NF_2$, whereas those of series **B** follow the order $-NH_2 < -NHNH_2 < -NHNO_2 < -NO_2 < -NF_2$. It can be concluded that the $-NF_2$ group contributes more than the other energetic groups, especially the $-NH_2$ and $-NHNH_2$ groups, in increasing the densities of the designed molecules. In view of the detonation velocity and detonation pressure, six compounds (**A2**, **A4**, **A5**, **B1**, **B2**, and **B4**) have higher detonation velocities than RDX and five compounds (**A2**, **A4**, **B1**, **B2**, and **B4**) have higher detonation pressures than HMX. For series **A**, compound **A1** substituted with a $-NO_2$ group has the lowest detonation velocity (8.47 km s^{-1}), whereas compound **B5** substituted with a $-NH_2$ group has the

Table 3. Predicted densities (ρ), heats of detonation (Q), detonation velocities (D), and detonation pressures (P) for the designed compounds.

Compd	Q [cal g^{-1}]	ρ_0 [g cm^{-3}]	ρ [g cm^{-3}]	D [km s^{-1}]	P [GPa]
A1	998.3	2.05	1.96	8.47	33.4
A2	2187.6	2.43	2.29	12.18	75.1
A3	1250.3	1.49	1.54	8.60	29.8
A4	1394.5	1.96	1.90	9.34	39.3
A5	1332.5	1.49	1.52	8.86	31.4
B1	1131.5	2.09	2.00	8.75	36.0
B2	2137.9	2.47	2.32	12.08	74.3
B3	781.9	1.43	1.48	7.29	20.8
B4	1435.1	1.97	1.90	9.24	39.0
B5	536.6	1.48	1.54	7.02	19.8
RDX	1591.0	–	1.82	8.75	34.0
HMX	1633.9	–	1.91	9.10	39.0

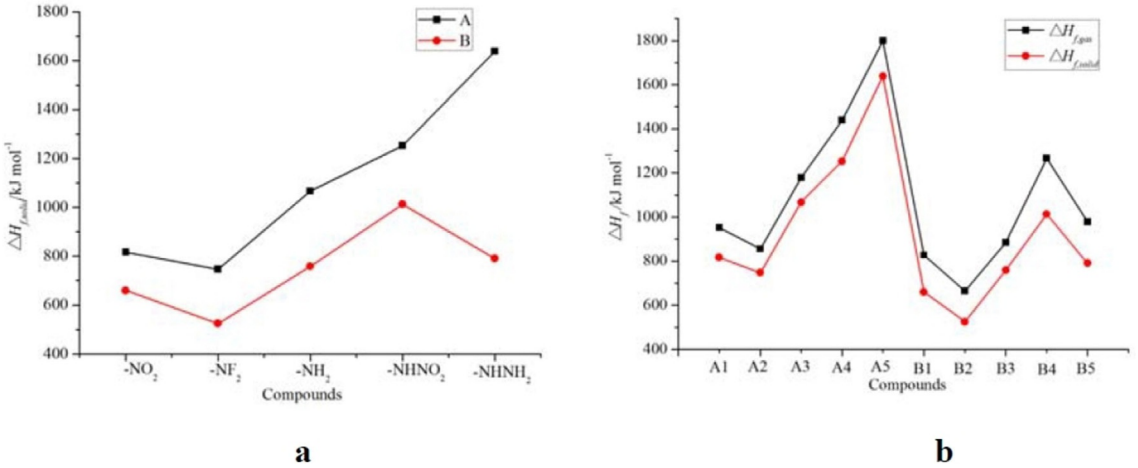

a b

Figure 3. Variation trends of Q, ρ, D, and P of the designed compounds.

lowest detonation pressure (29.8 GPa). However, for series **B**, compound **B5** substituted by a $-NHNH_2$ group has the lowest detonation properties ($D = 7.02\ km\ s^{-1}$ and $P = 19.8$ GPa). Notably, compound **A2** (substituted by a $-NF_2$ group) has remarkable detonation properties with $D = 12.18\ km\ s^{-1}$ and $P = 75.1$ GPa. This is consistent with our previous research in which it was shown that the $-NF_2$ group was effective in improving the Q, ρ, D, and P values of an energetic material, whereas the $-NH_2$ and $-NHNH_2$ groups only slightly contributed to these values.[12]

2.3. Thermal Stability and Sensitivity

The bond dissociation energy (BDE) and the drop height $h_{50\%}$ (H_{50}) are the most commonly used methods to assess the thermal stability and impact sensitivity of energetic materials.[13–15] In general, small bond dissociation energy and impact sensitivity values are indicative of bonds that are easy to break and molecules that have low stability. People nowadays have reached a consensus that the energetic groups attached to the parent compounds often act as the primary source to initiate the reactivity of organic energetic compounds. Therefore, the bond order and bond dissociation energies of the weakest N–R, C–R, NH–NH_2, and NH–NO_2 bonds were investigated, and the results are summarized in Table 4. Also, the H_{50} data are listed to evaluate the impact sensitivities of the designed compounds. From Table 4 it is found that the bond orders of the N–R bond of series **A** and **B** lie in the ranges of 0.6799 (for **A1**) to 1.0282 (for **A2**) and 0.6810 (for **B1**) to 1.0356 (for **B2**), whereas the bond order of the C–R bond of series **B** ranges from 0.8880to 1.1175. On the whole, the bond orders of the C–R bonds are much higher than those of the N–R bonds. In view of the bond dissociation energies and impact sensitivities, all of the designed compounds have moderate values ranging from 0.8 to 104.9 $kJ\ mol^{-1}$ and from 7.4 to 52.7 cm, respectively.

Figure 4 presents the variation trends of the bond order (BO), BDE without ZPE correction (BDE_0), BDE with ZPE correction (BDE_{ZPE}), and H_{50} of the designed compounds. First (Figure 4a), the bond order of series **A** follows the order $-NO_2 < -NHNH_2 < -NH_2 < -NHNO_2 < -NF_2$. However, for series **B**, the bond order of the N–R bond follows the order $-NO_2 < -NHNH_2 < -NHNO_2 < -NH_2 < -NF_2$, whereas that of the C–R bond follows the order $-NO_2 < -NF_2 < -NHNO_2 < -NHNH_2 < -NH_2$. However, the bond order should not be conclusive in estimating the thermal stability of an energetic material, and thus, the bond dissociation energies were calculated and are shown in Figure 4b,c. It is found that the BDE_0 values are larger than the BDE_{ZPE} values. For series **A**, the BDE_{ZPE} values follow the order $-NO_2 < -NHNH_2 < -NF_2 < -NH_2 < -NHNO_2$, and for series **B**, these values follow the order $-NO_2 < -NF_2 < -NHNH_2 < -NHNO_2 < -NH_2$. It is also found that the bonds of the designed compounds (except for compound **B4**) that trigger thermal decomposition are the N–R bonds and not the C–R bonds, which may be due to the high energy of the C–R chemical bonds. Notably, we selected the weakest bond dissociation energy, and the corresponding bond order is shown in Figure 4a. Taking compound **B4** as an example, three kinds of thermal-decomposition-triggering bonds are located in the molecule (N–R, C–R, and NH–NO_2), and the NH–NO_2 bond possesses the lowest bond dissociation energy. Therefore, the bond dissociation energy of the NH–NO_2 bond and the corresponding bond order were selected and are drawn in Figure 4. As for H_{50}, series **A** follows the sequence $-NHNH_2 < -NH_2 < -NO_2 < -NF_2 < NHNO_2$, whereas series **B** follows the order $-NH_2 < -NO_2 < -NHNH_2 < -NF_2 < -NHNO_2$. Thus, compounds substituted with a $-NHNO_2$ group are the most insensitive to external stimuli. This may be a result of intramolecular hydrogen bonds (Figure 5, H···O),[16] which can clearly decrease the sensitivity.

In terms of the detonation properties, thermal stabilities,[17] and impact sensitivities, compounds **A4** ($D = 9.34\ km\ s^{-1}$, $P = 39.3$ GPa. $H_{50} = 52.7$ cm) and **B4** ($D = 9.24\ km\ s^{-1}$, $P = 39.0$ GPa, $H_{50} = 45.1$ cm) were finally screened as potential high-energy-density materials because their detonation properties and sensitivities are superior to those of RDX ($D = 8.75\ km\ s^{-1}$, $P = 34.0$ GPa, $H_{50} = 26$ cm) and HMX ($D = 9.1\ km\ s^{-1}$, $P = 39.0$ GPa, $H_{50} = 29$ cm).[11] The frontier molecular orbitals, electronic densities, electrostatic potentials, and thermal dynamic properties of compounds **A4** and **B4** were also investigated to give a better understanding of the physical and chemical properties of these promising high-energy-density materials.

Table 4. Bond dissociation energies and impact sensitivities of the designed compounds.

Compd	BO N–R	BDE_0 [$kJ\ mol^{-1}$]	BDE_{ZPE} [$kJ\ mol^{-1}$]	BO C–R	BDE_0 [$kJ\ mol^{-1}$]	BDE_{ZPE} [$kJ\ mol^{-1}$]	BO $NH–NO_2$ or $NH–NH_2$	BDE_0 [$kJ\ mol^{-1}$]	BDE_{ZPE} [$kJ\ mol^{-1}$]	H_{50} [cm]
A1	0.6799	19.7	6.9	–	–	–	–	–	–	24.2
A2	1.0282	33.5	20.1	–	–	–	–	–	–	51.1
A3	1.0090	109.3	80.8	–	–	–	–	–	–	16.2
A4	1.0211	109.1	88.9	–	–	–	0.9009	121.2	104.1	52.7
A5	0.8892	37.3	19.7	–	–	–	1.0384	270.9	128.7	7.4
B1	0.6810	13.7	0.8	0.8880	223.9	207.7	–	–	–	9.8
B2	1.0356	36.3	22.4	1.0126	242.0	227.8	–	–	–	39.1
B3	1.0143	131.8	104.9	1.1175	443.6	411.6	–	–	–	9.5
B4	1.0026	131.2	109.9	1.0320	415.2	388.8	0.9082	118.8	100.8	45.1
B5	0.9196	61.4	43.9	1.1040	330.5	307.4	1.0295	183.8	151.9	24.2

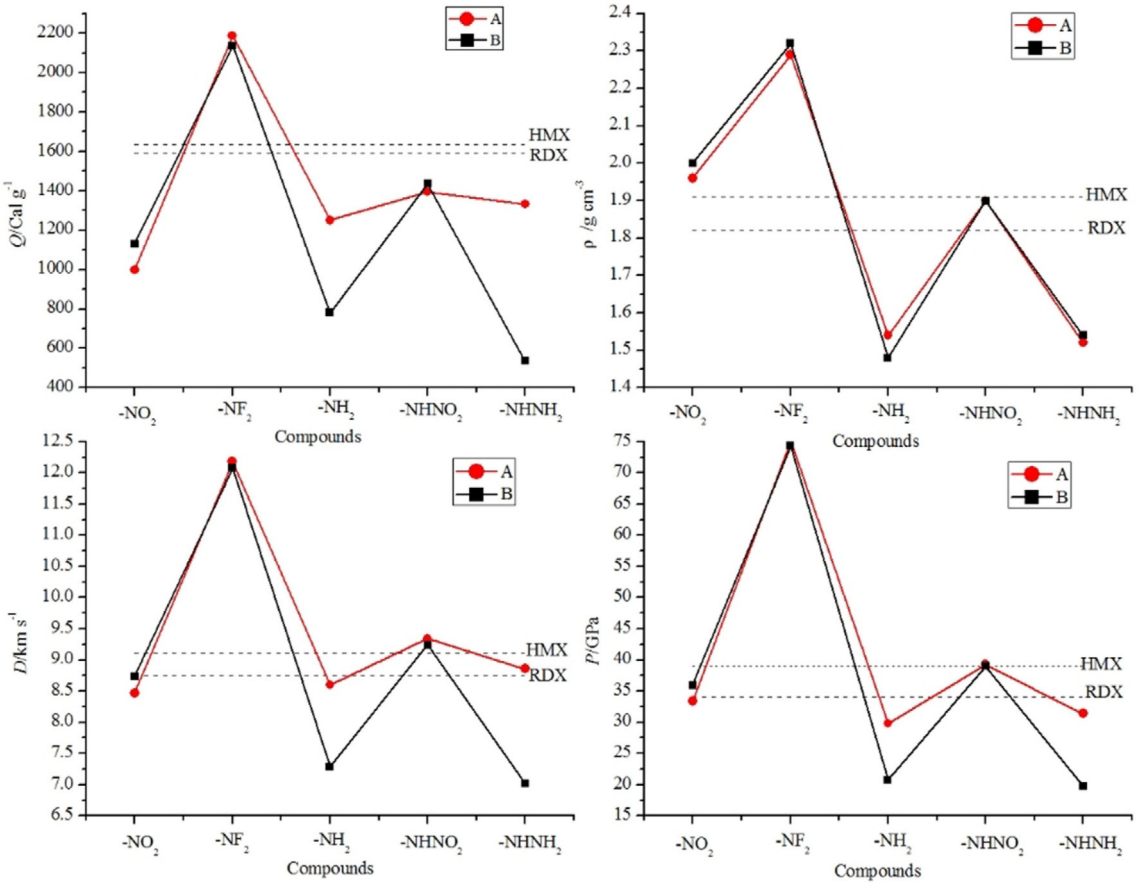

Figure 4. Variation trends of the BO, BDE_0, BDE_{ZPE}, and H_{50} of the designed compounds.

2.4. Frontier Molecular Orbitals

The highest occupied molecular orbital (HOMO) and the lowest unoccupied molecular orbital (LUMO) are two important aspects for frontier molecular orbitals.[18,19] Besides the orbitals, the energy gap between the HOMO and LUMO is commonly investigated, as it can determine the kinetic stability, chemical reactivity, and optical polarizability of an energetic material. The distribution of the HOMO and LUMO combined with their energy gap are depicted in Figure 5. As can be seen, the distribution of the HOMO and LUMO of compound **A4** varies from that of compound **B4** due to the electronic effect of the different parent structures. For compound **A4**, the LUMO (MO = 121) is mostly localized on the whole surface of the molecule, whereas the HOMO (MO = 120) is approximately localized on the parent structure of the molecule and partially distributed on the $-NHNO_2$ group (Figure 6). For compound **B4**, the LUMO (MO = 151) is mainly localized on the right part of the molecule, whereas the HOMO (MO = 150) is mainly localized on the tetrazine ring. In addition, the calculated energy gaps between the HOMO and LUMO for compounds **A4** and **B4** are 5.82 and 4.60 eV, respectively. It can be inferred from the energy gap that compound **B4** has higher chemical reactivity than compound **A4** under external stimuli.

2.5. Electronic Density

Electronic density is a fundamental indicator that can express various physical and chemical properties of an energetic material.[20,21] The contour line maps of the electronic densities on compounds **A4** and **B4** are visualized in Figure 7. In the figure, high peaks correspond to the nuclear charge of a heavy nucleus, which improves electron aggregation. It can be seen from the picture that the electron densities around the presented atoms follow the sequence oxygen atom > nitrogen atom > carbon atom > hydrogen atom. Clearly, the electron densities around the oxygen atoms are the highest due to their strong electron absorption effects. Moreover, due to the fact that the electron pair is shared between atoms with covalent interactions, the electrons are mainly assembled in the bonding area, especially in the double-bonding area (such as regions A1 and A2 in compound **A4** and regions B1 and B2 in compound **B4**). These areas suggest that covalent bonding is derived from the π orbitals over the C=C and C=N bonds. On the other hand, delocalization also occurs in the tetrazine ring (region A3 in compound **A4** and region B3 in compound **B4**), which may improve the stability of the ring skeleton and the molecular structure. Again, for compound **B4**, regions B4 and B5 are electron delocalized, which may be due to intramolecular hydrogen bonds between O(M)···H(N) and O(P)···H(Q). In addition, electronic density is reduced in regions A4 and B6 be-

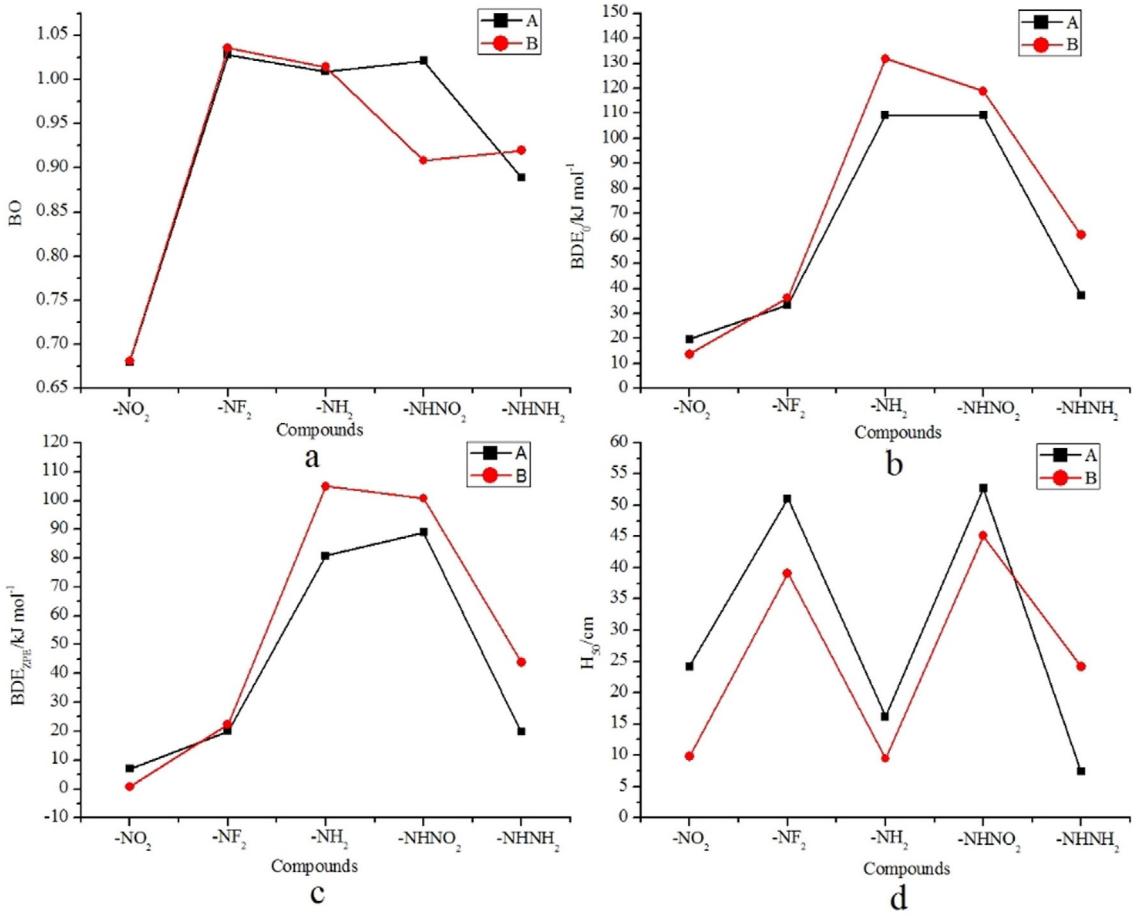

Figure 5. Intramolecular hydrogen bonds of compounds **A4** and **B4**.

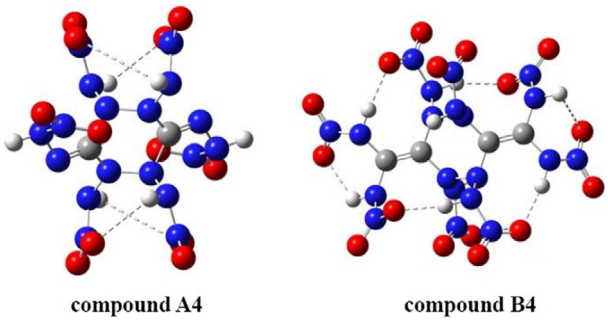

Figure 6. HOMOs and LUMOs of compounds **A4** and **B4**.

cause of the repulsive interactions of the lone pair of electrons among the adjacent atoms.

2.6. Electrostatic Potential

The electrostatic potential (ESP) is an integral part in investigating the intermolecular interaction, charge distributions, and chemical reactivity sites on molecular surfaces.[22,23] The critical data of the electrostatic potential for compounds **A4** and **B4** were obtained by using the Multiwfn program. The molecular ESPs calculated at the B3LYP/6-31G(d,p) level are depicted in

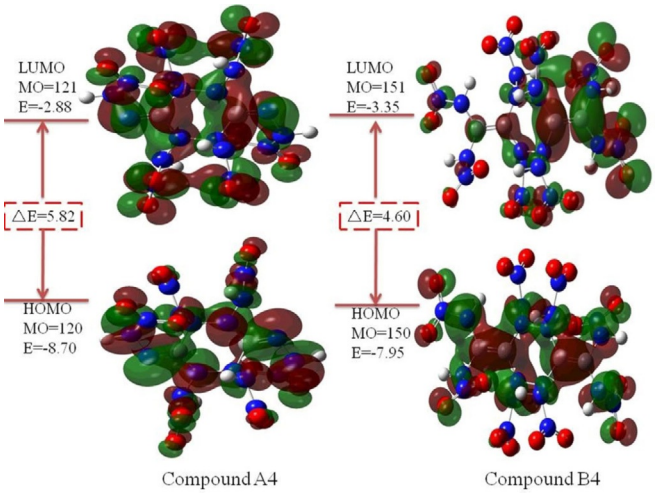

Figure 7. Contour line maps of compounds **A4** and **B4**.

Figure 8; the red color denotes the most negative potential, whereas the blue color denotes the most positive potential. Again, the ratios of the surface areas in each ESP range are also visualized in Figure 8. From the figure it can be seen that the negative potentials are mainly distributed on $-NHNO_2$,

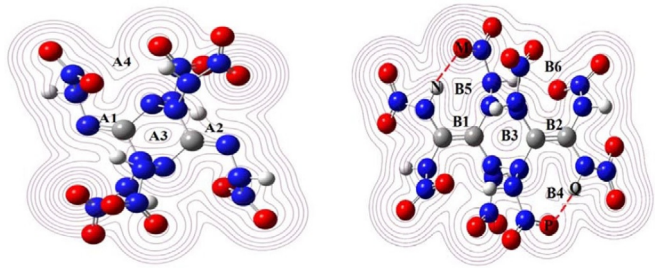

Figure 8. Electrostatic potentials of compounds **A4** and **B4**.

whereas the positive potentials are mostly localized in the center of the cyclic skeleton. This distribution style stabilizes the parent structure, which in turn improves the stability of the energetic molecule. In addition, the global maxima and minima of the ESPs of compounds **A4** and **B4** were also calculated. The global maxima ESPs of compounds **A4** and **B4** are +57.36 and +64.76 kcal mol^{-1}, whereas the global minima ESPs of compounds **A4** and **B4** are −19.65 and −16.31 kcal mol^{-1}, respectively. Upon inspection of the surface areas of the positive and negative potentials, it is found that the positive potential areas of compounds **A4** and **B4** are 168.44 (ratio 52.9%) and 200.20 Å^2 (ratio 54.23%), respectively. Clearly, the areas of the positive potentials on compounds **A4** and **B4** are larger than the areas of the negative potentials. Klapötke et al. proposed that energetic materials with positive potentials that are centralized and large will be more stable.[24] Not surprisingly, the ESPs of compounds **A4** and **B4** agree well with this hypothesis.

2.7. Thermal Dynamic Properties

The thermal dynamic properties, such as standard molar heat capacity ($C^{\theta}_{p,m}$), standard molar entropy (S^{θ}_{m}), and standard molar thermal enthalpy (H^{θ}_{m}) from 200 to 600 K were calculated on the basis of vibrational analysis. The relationships between these thermodynamic functions and the temperatures of compounds **A4** and **B4** were also done by nonlinear fitting. For compound **A4**, the equations for $C^{\theta}_{p,m}$ [Eq. (1)], S^{θ}_{m} [Eq. (2)], and H^{θ}_{m} [Eq. (3)] can be written as follows:

$$C^{\theta}_{p,m} = 57.17 + 1.55\,T - 0.00090\,T^2 \quad R^2 = 0.9999 \quad (1)$$

$$S^{\theta}_{m} = 321.69 + 1.87\,T - 0.000657\,T^2 \quad R^2 = 0.9999 \quad (2)$$

$$H^{\theta}_{m} = -14.63 + 0.19\,T + 0.000414\,T^2 \quad R^2 = 0.9999 \quad (3)$$

and for compound **B4**, they can be written as follows [Eqs. (4), (5), and (6)]:

$$C^{\theta}_{p,m} = 69.89 + 1.92\,T - 0.00109\,T^2 \quad R^2 = 0.9999 \quad (4)$$

$$S^{\theta}_{m} = 359.21 + 2.31\,T - 0.00793\,T^2 \quad R^2 = 0.9999 \quad (5)$$

$$H^{\theta}_{m} = -16.96 + 0.23\,T + 0.000527\,T^2 \quad R^2 = 0.9999 \quad (6)$$

Figure 9 displays the variation trends of $C^{\theta}_{p,m}$, S^{θ}_{m}, and H^{θ}_{m}. It is found that the thermodynamic properties improve markedly upon increasing the temperature. However, the rates by which $C^{\theta}_{p,m}$ and S^{θ}_{m} increase become slower, whereas the rate by which H^{θ}_{m} increases is distinct. This is because the translations and rotations of a molecule have the most impact at low temperatures, whereas the vibrational motion intensifies at higher temperatures and makes more contributions to these compounds.[25,26] All of the parameters may provide useful information in further investigations of the equation of states and the chemical and physical properties of compounds **A4** and **B4**.

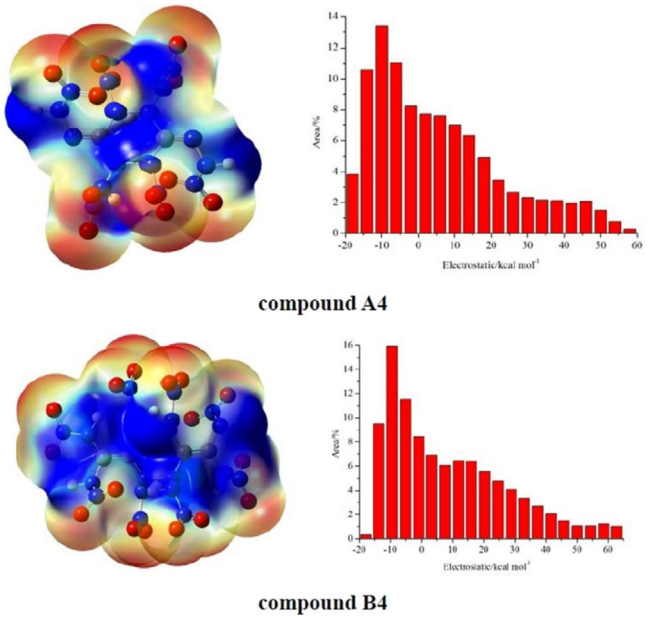

Figure 9. Relationships between the thermodynamic functions and temperature for compounds **A4** and **B4**.

3. Conclusions

In the presented work, ten novel substituted 1,2,4,5-tetrahydro-1,2,4,5-tetrazine energetic compounds were designed, and their chemical and physical properties were investigated. The results show that the parent molecules and designed compounds have high positive heats of formation. The effects of different substituents on the density, detonation velocity, and detonation pressure showed that the $-NF_2$ group was the most effective in improving the detonation properties, whereas the $-NH_2$ group may contribute less to these aspects. In view of the thermal stabilities and impact sensitivities, all of the compounds possess moderate bond dissociation energies (from 0.8 to 104.9 kJ mol^{-1}) and impact sensitivities (H_{50} = 7.4–52.7 cm). Taking both the detonation properties and stabilities into consideration, compounds **A4** and **B4** were selected as potential high-energy-density materials. Additionally, the frontier molecular orbitals, electronic densities, electrostatic potentials, and thermal dynamic parameters of compounds **A4** and **B4** were simulated, and it was found that they both have stable molecular structures.

Computational Methods

The B3LYP/6-31G(d,p) basis set of density functional theory (DFT) combined with Gaussian 03 software[27] were employed to optimize the geometries, predict the accurate energies, and simulate the vibrational frequencies of the designed compounds. All the optimized structures were characterized to be energy minima on the potential energy surface by vibrational analysis without the presence of imaginary frequencies.

The heat of formation (HOF) is critical for energetic compounds, as it is basic data to calculate the energetic properties, such as heat of detonation (Q), detonation velocity (D), and detonation pressure (P). However, to obtain HOFs by experimental methods would be dangerous and time consuming. Consequently, isodesmic reactions[28,29] were employed to calculate accurate HOFs of the designed compounds. This is because in the isodesmic reactions, the electronic circumstances of the related reactants and products are very similar, which in turn reduces the errors of the calculated HOF greatly.[30,31] The related isodesmic reactions (Figure 10) and equations [Eq. (7) and (8)] are as follows:

$$\Delta H_{298K} = \sum \Delta H_{f,p} - \sum \Delta H_{f,R} \quad (7)$$

$$\Delta H_{298K} = \Delta E_{298K} + \Delta(PV) = \Delta E_0 + \Delta ZPE + \Delta H_T + \Delta nRT \quad (8)$$

in which ΔH_{298K} is the HOF that needs to be calculated, $\Delta H_{f,p}$ and $\Delta H_{f,R}$ are the HOFs of the products and reactants, ΔE_0 is the energy change between the products and reactants, ΔZPE is the difference between the zero-point energies (ZPEs) of the products and reactants, ΔH_T is the thermal correction from 0 to298 K, n is the number of the energetic groups, and $\Delta(PV)$ is equal to ΔnRT.

In the isodesmic reactions, the HOFs of CH_4, NH_3, CH_3NHNH_2, CH_3NH_2, and CH_3NO_2 were available from the internet (https://webbook.nist.gov), whereas the HOFs of CH_3NF_2, CH_3NHNO_2, NH_2NF_2, NH_2NH_2, NH_2NHNH_2, NH_2NHNO_2, NH_2NO_2, 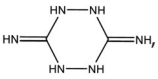 , and 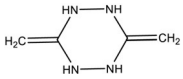 were unavailable. Therefore, the atomization reaction [Eq. (9)]:

$$C_aH_bN_c \rightarrow aC_{(g)} + bH_{(g)} + cN_{(g)} \quad (9)$$

was employed to evaluate the HOFs of these unknown compounds at the CBS-Q level.[32]

Generally, the condensed phases for most energetic compounds were solid, whereas the HOFs calculated from the above method were in the gas phase. Therefore, solid-phase HOFs were calculated according to Hess' law of constant heat summation [Eq. (10)]:[33]

$$\Delta H_{f,solid} = \Delta H_{f,gas} - \Delta H_{sub} \quad (10)$$

in which ΔH_{sub} is the heat of sublimation proposed by Politzer et al. It was found that the value of ΔH_{sub} correlated well with the molecular surface area (A) and the electrostatic interaction index ($\nu\sigma_{tot}^2$) for energetic compounds. The empirical expression of the approach can be written as follows [Eq. (11)]:[34]

$$\Delta H_{sub} = aA^2 + b(\nu\sigma_{tot}^2)^{0.5} + c \quad (11)$$

in which, a, b, and c are coefficients obtained from ref. [35], A is the surface area of the 0.001 e bohr^{-3} isosurface of electronic density of the molecule, ν is the degree of balance between the positive and negative potentials on the isosurface, and σ_{tot}^2 is the measure of variability of the electrostatic potential on the molecular surface, which can be obtained by the Multiwfn program.[36]

The accurate theoretical densities (ρ) were calculated by an improved method proposed by Politzer et al., and the equation was introduced as follows [Eq. (12)]:[22]

$$\rho = \beta_1\left(\frac{M}{V}\right) + \beta_2(\nu\sigma_{tot}^2) + \beta_3 \quad (12)$$

in which β_1, β_2, and β_3 are coefficients; M is the molecular mass [g mol^{-1}]; V is the volume of a molecule; ν is the degree of balance between the positive and negative potentials on the isosurface; and σ_{tot}^2 is a measure of variability of the electrostatic potential on the molecular surface.

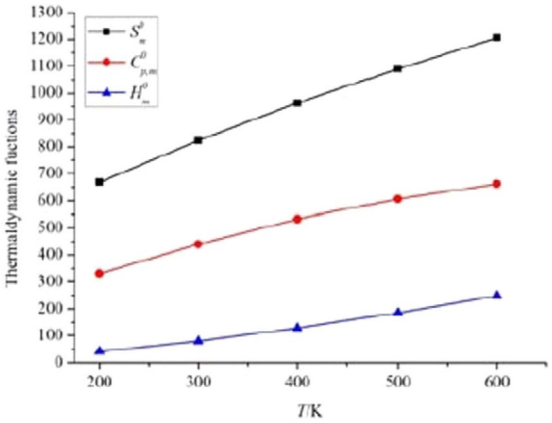

compound A4

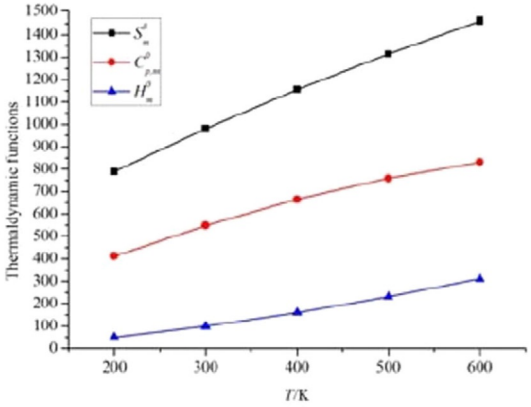

compound B4

Figure 10. Isodesmic reactions of the designed compounds.

On the basis of the densities and heats of formation, the corresponding detonation values were estimated by using the Kamlet–Jacobs equations [Eq. (13) and (14)]:[37]

$$D = 1.01(N\overline{M}^{0.5}Q^{0.5})^{0.5}(1 + 1.3\rho) \quad (13)$$

$$P = 1.558\rho^2 N\overline{M}^{0.5}Q^{0.5} \quad (14)$$

in which D is the detonation velocity [km s^{-1}]; P is the detonation pressure [GPa]; and N, $\overline{M}$, and Q are the moles of detonation gas per gram explosive [mol g^{-1}], the average molecular weight of these gases [g mol^{-1}], and the heat of detonation [cal g^{-1}], respectively.

The strength of bonding, which can be evaluated by the bond dissociation energy (BDE), is a fundamental indicator to investigate chemical processes of an energetic material (such as the way of bond cleavage, the thermal stability, and thermal decomposition mechanism). The homolytic bond dissociation energy is given in terms of [Eq. (15)]:

$$BDE_0(A{-}B) = E_0(A^{\bullet}) + E_0(B^{\bullet}) - E_0(A{-}B) \quad (15)$$

The bond dissociation energy with zero-point energy (ZPE) is also given to obtain accurate data for the bond dissociation energy based on the corrected equation [Eq. (16)]:

$$BDE(A{-}B)_{ZPE} = BDE_0(A{-}B) + \Delta E_{ZPE} \quad (16)$$

in which ΔE_{ZPE} is the difference between the ZPEs of the products and reactants.

Apart from the BDE, the impact sensitivity (H_{50}) was calculated due to its significance in predicting the impact stability of an energetic material [Eq. (17)].[38]

$$h_{50} = a\sigma_+^2 + b\frac{\sigma_+^2\sigma_-^2}{(\sigma_+^2 + \sigma_-^2)^2} + c \quad (17)$$

in which a, b, and c are constants and σ_+^2 and σ_-^2 are indicators of the strengths and variabilities of the positive and negative surface potentials.

Acknowledgements

This study was supported by the National Natural Science Foundation of China (Grant No. 11602121).

Conflict of Interest

The authors declare no conflict of interest.

Keywords: density functional calculations · detonation properties · electronic structure · energetic materials · nitrogen heterocycles

[1] T. M. Klapötke, T. G. Witkowski, *ChemPlusChem* **2016**, *81*, 357–360.
[2] A. K. Sikder, N. Sikder, *J. Hazard. Mater.* **2004**, *112*, 1–15.
[3] X. H. Jin, J. H. Zhou, S. J. Wang, B. C. Hu, *Quim. Nova* **2016**, *39*, 467–473.
[4] D. M. Badgujar, M. B. Talawar, P. P. Mahulikar, *Cent. Eur. J. Energ. Mater.* **2017**, *14*, 821–843.
[5] X. H. Jin, J. H. Zhou, B. C. Hu, C. M. Ma, *J. Phys. Org. Chem.* **2017**, *30*, e3704.
[6] D. E. Chavez, S. K. Hanson, J. M. Veauthier, D. A. Parrish, *Angew. Chem. Int. Ed.* **2013**, *125*, 7014–7017; *Angew. Chem.* **2013**, *125*, 7152–7155.
[7] T. Wei, W. H. Zhu, X. W. Zhang, Y. F. Li, H. M. Xiao, *J. Phys. Chem. A* **2009**, *113*, 9404–9412.
[8] A. Saikia, R. Sivabalan, B. G. Polke, G. M. Gore, A. Singh, A. S. Rao, A. K. Sikder, *J. Hazard. Mater.* **2009**, *170*, 306–313.
[9] M. H. V. Huynh, M. A. Hiskey, E. L. Hartline, D. P. Montoya, R. Montoya, *Angew. Chem. Int. Ed.* **2004**, *43*, 4924–4928; *Angew. Chem.* **2004**, *116*, 5032–5036.
[10] Q. Wu, W. H. Zhu, H. M. Xiao, *J. Chem. Eng. Data* **2013**, *58*, 2748–2762.
[11] T. Yan, W. J. Chi, J. Bai, L. L. Li, B. T. Li, H. S. Wu, *J. Mol. Model.* **2013**, *19*, 2235–2242.
[12] X. H. Jin, L. Wang, Y. Tan, J. Ren, Z. M. Wang, Y. L. Liu, L. Y. Wang, J. H. Zhou, B. C. Hu, *ChemistrySelect* **2018**, *3*, 1142–1150.
[13] Q. L. Yan, S. Zeman, *Int. J. Quantum Chem.* **2013**, *113*, 1049–1061.
[14] S. Zeman, Jungova, *Propellants Explos. Pyrotech.* **2016**, *41*, 426–451.
[15] Z. Yu, E. R. Bernstein, *J. Phys. Chem. A* **2013**, *117*, 10889–10902.
[16] X. H. Jin, B. C. Hu, *Z. Anorg. Allg. Chem.* **2016**, *642*, 635–642.
[17] G. S. Chung, M. W. Schmidt, M. S. Gordon, *J. Phys. Chem. A* **2000**, *104*, 5647–5650.
[18] G. C. Yang, H. L. Hu, Y. Zhou, Y. J. Hu, H. Huang, F. D. Nie, W. M. Shi, *Sci. Rep.* **2012**, *2*, 698.
[19] P. He, J. G. Zhang, K. Wang, X. Yin, X. Jin, T. L. Zhang, *Phys. Chem. Chem. Phys.* **2015**, *17*, 5840–5848.
[20] P. He, J. G. Zhang, K. Wang, X. Yin, T. L. Zhang, *J. Org. Chem.* **2015**, *80*, 5643–5651.
[21] P. Politzer, P. Lane, J. S. Murray, *Cent. Eur. J. Energ. Mater.* **2013**, *10*, 37–52.
[22] P. Politzer, J. Martinez, J. S. Murray, M. C. Concha, A. Toro-Labbé, *Mol. Phys.* **2009**, *107*, 2095–2101.
[23] G. Z. Zhao, M. Lu, *J. Phys. Org. Chem.* **2014**, *27*, 10–17.
[24] A. Hammerl, T. M. Klapötke, H. Nöth, M. Warchhold, G. Holl, *Propellants Explos. Pyrotech.* **2003**, *28*, 165–173.
[25] Q. Wu, W. H. Zhu, H. M. Xiao, *J. Mater. Chem. A* **2014**, *2*, 13006–13015.
[26] J. Zhang, H. M. Xiao, *J. Chem. Phys.* **2002**, *116*, 10674–10683.
[27] Gaussian 03, Revision D.01, M. J. Frisch, G. W. Trucks, H. B. Schlegel, G. E. Scuseria, M. A. Robb, J. R. Cheeseman, J. A. Montgomery, T. Vreven, K. N. Kudin, J. C. Burant, J. M. Millam, S. S. Iyengar, J. Tomasi, V. Barone, B. Mennucci, M. Cossi, G. Scalmani, N. Rega, G. A. Petersson, H. Nakatsuji, M. Hada, M. Ehara, K. Toyota, R. Fukuda, J. Hasegawa, M. Ishida, T. Nakajima, Y. Honda, O. Kitao, H. Nakai, M. Klene, X. Li, J. E. Knox, H. P. Hratchian, J. B. Cross, C. Adamo, J. Jaramillo, R. Gomperts, R. E. Stratmann, O. Yazyev, A. J. Austin, R. Cammi, C. Pomelli, J. W. Ochterski, P. Y. Ayala, K. Morokuma, G. A. Voth, P. Salvador, J. J. Dannenberg, V. G. Zakrzewski, S. Dapprich, A. D. Daniels, M. C. Strain, O. Farkas, D. K. Malick, A. D. Rabuck, K. Raghavachari, J. B. Foresman, J. V. Ortiz, Q. Cui, A. G. Baboul, S. Clifford, J. Cioslowski, B. B. Stefanov, G. Liu, A. Liashenko, P. Piskorz, I. Komaromi, R. L. Martin, D. J. Fox, T. Keith, M. A. Al-Laham, C. Y. Peng, A. Nanayakkara, M. Challacombe, P. M. W. Gill, B. Johnson, W. Chen, M. W. Wong, C. Gonzalez, J. A. Pople, Gaussian, Inc., Pittsburgh, PA, **2003**.
[28] Y. Y. Guo, W. J. Chi, Z. S. Li, Q. S. Li, *RSC Adv.* **2015**, *5*, 38048–38055.
[29] Q. Wu, Y. Pan, X. L. Xia, Y. L. Shao, W. H. Zhu, H. M. Xiao, *Struct. Chem.* **2013**, *24*, 1579–1590.
[30] Q. Wu, W. H. Zhu, H. M. Xiao, *J. Mol. Model.* **2013**, *19*, 2945–2954.
[31] Y. H. Joo, B. Twamley, S. Garg, J. M. Shreeve, *Angew. Chem. Int. Ed.* **2008**, *47*, 6332–6335; *Angew. Chem.* **2008**, *120*, 6332–6335.
[32] F. Wang, G. X. Wang, H. C. Du, J. Y. Zhang, X. D. Gong, *J. Phys. Chem. A* **2011**, *115*, 13858–13864.
[33] P. W. Atkins, *Physical Chemistry*, 2nd ed., Oxford University Press, Oxford, **1982**.
[34] P. Politzer, Y. Ma, P. Lane, M. C. Concha, *Int. J. Quantum Chem.* **2005**, *105*, 341–347.
[35] E. F. C. Byrd, B. M. Rice, *J. Phys. Chem. A* **2006**, *110*, 1005–1013.
[36] T. Lu, F. Chen, *J. Comput. Chem.* **2012**, *33*, 580–592.
[37] M. J. Kamlet, S. J. Jacobs, *J. Chem. Phys.* **1968**, *48*, 23–25.
[38] M. Pospisil, P. Vávra, M. C. Concha, J. S. Murray, P. Politzer, *J. Mol. Model.* **2010**, *16*, 895–901.

Received: August 6, 2018
Revised manuscript received: August 19, 2018

